Chapter 10

Design, Synthesis, and Fabrication of a Novel Self-Assembling Fibrillar Protein

J. P. O'Brien[1], R. H. Hoess[2], K. H. Gardner[3], R. L. Lock[1], Z. R. Wasserman[4], Patricia C. Weber[4], and F. R. Salemme[5]

[1]DuPont Fibers, Experimental Station, Wilmington, DE 19880–0302
[2]DuPont Merck Pharmaceuticals, Experimental Station, Wilmington, DE 19880–0328
[3]DuPont Central Research and Development, Experimental Station, Wilmington, DE 19880–0356
[4]DuPont Merck Pharmaceuticals, Experimental Station, Wilmington, DE 19880–0228
[5]3-Dimensional Pharmaceuticals, Kennett Square, PA 19348–2705

Evolution has yielded a host of biopolymers and biomaterials with highly sophisticated structural organization at the molecular level. An elegant, but comparatively simple, example of such advanced structural organization is found in the fibrillar spikes protruding from the capsids of adenovirus serotypes. The shaft portion of these viral spikes is assembled from three identical protein strands and resembles a cylindrical or box beam on the molecular level. We report here the design, synthesis, and characterization of recombinant protein polymers based on multimers of 15 amino acid consensus sequences approximating the more complex natural protein. Spontaneous fibrillar aggregate formation in the genetically engineered analogs has been confirmed by various methods and the propensity of such aggregates to phase separate into liquid crystalline arrays has been observed. Moreover, it has been possible to spin filaments from liquid crystalline solutions and characterize their structure. The collective data provide what we believe is the first example of a recombinant biopolymer capable of self-organization to rigid, high-aspect-ratio assemblies suitable for anisotropic solution processing.

Polymer and materials researchers are increasingly looking to natural materials as paradigms for the design and synthesis of a new generation of structural materials. With the advent of genetic engineering methodology, it is now possible to harness polymer biosynthesis in certain biopolymer classes to control the properties and functionality of synthetic materials. Operating from a belief that future materials systems will provide value by offering efficient, specific solutions to complex material needs, this work was undertaken, in part, to determine the feasibility of synthetically replicating a sophisticated, natural polymer fiber assembly for possible commercial applications.

Figure 1 is a schematic illustration of a human serotype adenovirus. The

0097–6156/94/0544–0104$06.00/0

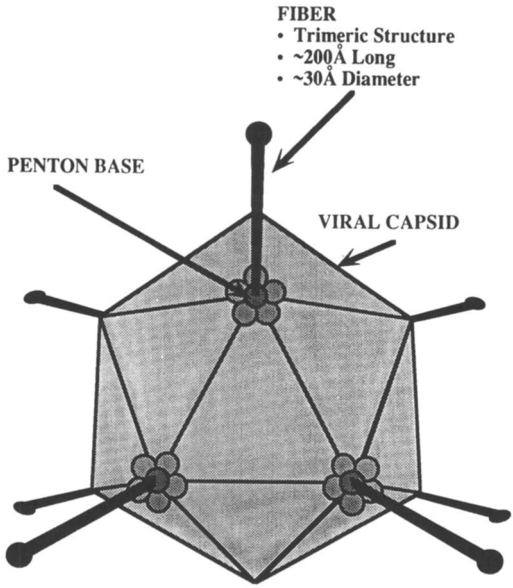

Figure 1. Schematic representation of a human adenovirus type 2 depicting placement of the capsid spikes and the approximate dimensions of the fibrillar shaft.

icosohedral capsid is featured with fibrillar spikes that emanate from 5-fold vertices (pentons) at 12 symmetrically distributed locations (*1*). The spikes, which are not covalently attached to the surface of the capsid are comprised of a shaft and a terminal globular structure, the latter of which is believed to mediate attachment of the virus to a host cell to facilitate the transfer of viral nucleic acids.

The shaft portion of the spike was of primary interest because of its apparent rigidity and the existence of prior evidence suggesting that it is comprised of a dimeric or trimeric assembly of protein molecules (*2,3*). Green et al. have suggested that the shaft proteins contain about 580 amino acid residues giving rise to a shaft length approaching 200Å. This is in agreement with previous electron diffraction studies and has been rationalized based on a model in which the proteins comprising each strand consist of ribbon-like, cross β structures containing short β strands flanked by β turns (*4*). More recently, Stouten et al. (*5*) has proposed a triple helical model for the adenovirus shaft based on features in the diffraction patterns obtained from single crystals of fiber (*6*). This model requires that individual protein strands be more chain extended than previously proposed.

Herisse et al. (*7,8*) sequenced the fibrillar region of human adenovirus type 2, leading to the identification of an uninterrupted reading frame coding for a protein polymer of mol. wt. of 62,000. Analysis of the sequence data suggested that the shaft portion of the fibrillar spike could be approximated by 15 residue consensus sequences having two short (3 residue) β strands and two alternating (4 and 5 residue) β turns.

Modeling, secondary structure analysis, and electron microscopy studies further suggested the existence of a long, narrow β sheet within the shaft region terminated by a shorter, but structurally more complex, knob region(*4*). Keying off these previous studies, we undertook synthesis of analogs of the shaft portion of adenovirus fibrillar protein via recombinant DNA methods. The constructs designed have exceptional structural regularity based on the precise repetition of monotonous 15 amino acid blocks in the polymer backbone. This approach is in contrast to previous work describing the cloning and expression of gene fragments isolated directly from adenovirus which code for the fiber portion of the gene(*9,10*). The overall approach in this work is depicted in Figure 2.

Design Considerations for Adenovirus-like Constructs

The fundamental design objective was to produce a material that could be spun into fibers with hierarchical molecular order, in which elements of structure present at the molecular level were aligned on the macroscopic scale of the fiber. A basic characteristic of natural assemblies and composites possessing hierarchical structural order is the temporal independence of structure formation at successive levels of the assembly organization. In the case of fibers, it has long been an objective to obtain fibrous materials where individual molecular polymer chains are aligned directly along the major fiber axis, an arrangement that realizes the ultimate material tensile properties. Such chain aligned order can be introduced by a variety of means, including post spin stretching or shear induced alignment from polymeric solutions. The latter process is substantially facilitated when individual polymer chains are rigid on the molecular scale, such that fibers possessing a high degree of chain alignment and associated superior mechanical properties result. Well known examples include the family of KEVLAR aramid polymers commercialized by DuPont.

In the context of the adenovirus constructs, the repetitive consensus sequence was designed to organize first as an assembly of three polypeptide chains that formed long rigid fibrils modeled on the natural adenovirus spike structural paradigm. Such fibrils might then be expected to have a high propensity for alignment when spun from concentrated solutions under appropriate solvent and concentration conditions. Since previous structural analysis had indicated that the natural structure possessed cross-beta sheet structure, an additional possibility was that post-spin processing

from the prealigned fibrillar aggregates could ultimately produce chain extended polypeptide structures, perhaps possessing the tensile characteristics of high performance polyethylene, but with added thermal stability conferred by interchain hydrogen bonding between backbone amide groups. As we demonstrate below, the constructs developed do polymerize to form rigid fibrillar structures that yield lyotropic liquid crystalline solutions which can be spun into fibers.

Modeling the Adenovirus Structure

The primary objective of the protein engineering effort was to use the underlying trimeric fibril as a scaffold for anchoring chemical functional groups whose order might be preserved up to the scale of the macroscopic fiber. This objective motivated modeling studies aimed at producing structures with improved properties and additional functionality. In developing this model we followed the initial suggestion of Green et al. (*4*) that individual chains were organized as independent cross-beta sheets, but also incorporated data suggesting that the fibril was composed of 3 polypeptide chains (*2,3*). It was assumed that each protein monomer would form a cross-beta sheet with the long axis of the monomer approximately perpendicular to that of the individual beta strands, which have good hydrogen bonding between them. In the fibril model, three slightly twisted cross-beta sheets have an interchain twist characteristic of that observed in proteins with antiparallel sheets of comparable extent. These are assembled into a threefold symmetric box beam with a cylindrical cross section where the edges of adjacent sheets are overlapping (Figure 3).

The box beam, as modeled, has a gentle left-handed helical twist. Although a pitch of 140Å, arises from the interchain sheet twist, and resembles the pitch of coiled-coil helical structural proteins like tropomyosin, slight variations in local interchain geometry are possible and could result in structures whose pitch may be considerably greater. In this conception, the interior of the beam is filled with hydrophobic amino acid side chains with charged and other hydrophilic amino acid side chains located on the outside surface of the beam. It is expected that intermolecular hydrogen bonding between polar side chains at the edges of the individual sheet contributes to the stability of the proposed structural organization. The model shown in Figure 3 was assembled in several stages, using a combination of interactive computer graphics, mathematical deformations, and minimization of the potential energy. Although the model was essentially built "ab initio," one can find small segments of X-ray crystallographic structures of natural proteins which match, on a local scale, segments from the computer model, indicating that there exists some similarity between the structure of this model and that of natural proteins.

Recent analysis of the diffraction patterns obtained from paracrystals of adenovirus spike protein (*5*) have suggested an alternative model for the shaft which differs from that shown in Figure 3. Specifically, it is essentially a three-start helical structure where sheet hydrogen bonds are almost exclusively formed between segments of different chains. However, in many respects this alternative structure retains a mass distribution and local chain orientation similar to the model shown in Figure 3. Further studies of the synthetic structures will hopefully reveal more detailed features of its organization.

Synthesis of Fiber Protein Analogs

To carry out the synthesis of these novel fibrillar proteins, a suitable vector for bacterial expression was required, as well as additional strategies for generating the synthetic genes necessary to encode the target polymers. Using recombinant DNA technology, we developed a strategy to produce protein polymers of sufficently high molecular weight with defined lengths and repetitive structural motifs.

As vectors for expression of protein biopolymers, a series of pBR322 derived plasmids, designated pRHF, were constructed (Figure 4). The salient feature of these plasmids is a cassette which includes a suitable restriction site for the insertion of

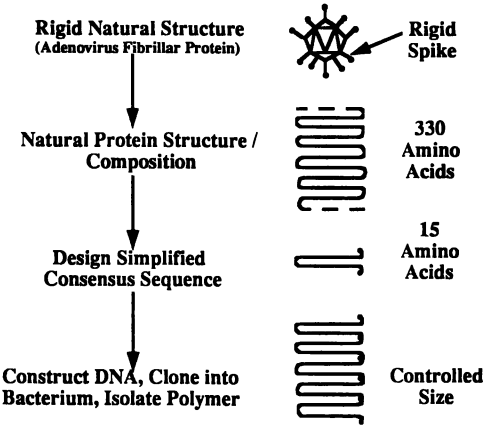

Figure 2. Overall approach to the design and synthesis of adenovirus fibrillar shaft proteins. The consensus sequences capture the basic structural elements of the more complex natural sequence.

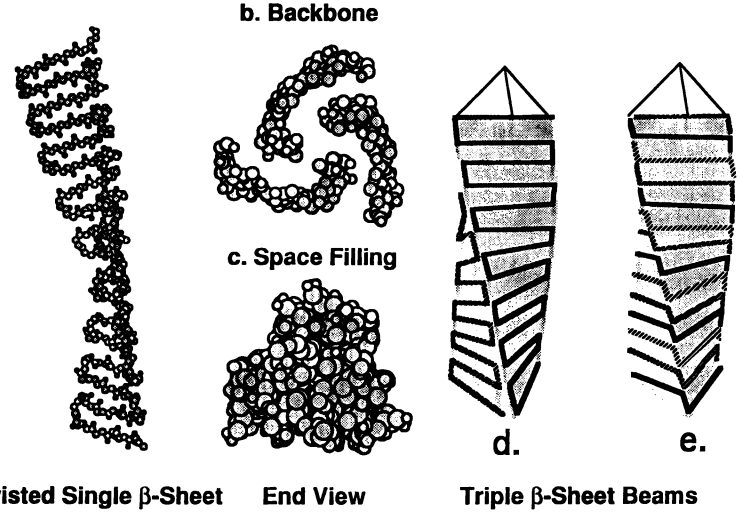

Figure 3. Computer-generated model of the target structure for the adenovirus fiber construct. a) One protein monomer, showing a backbone tracing. b) Endview of the trimeric backbone structure showing the sheet overlap. c) Endview of the trimeric space-filling structure illustrating the compact interior packing. d) A fibril schematic illustrating the chain arrangement modeled here. e) An approximate representation of the alternative structure derived in (*5*).

DNA coding for the biopolymer and the controlling sequences necessary for high levels of expression of the cloned insert. Since the synthetic biopolymer has the potential for being toxic to the host bacterium *Escherichia coli*, a conditional expression system was utilized so that construction of the gene could be completed in the absence of any expression. Once the construction of the gene was complete, the plasmid could then be transferred to a different bacterial host which would allow for expression. This precautionary measure serves to circumvent selective pressures against a gene expressing a potentially toxic gene product, and thus avoid the complication of unwanted deletions or rearrangements of the coding sequence. The sequences controlling expression of the biopolymer gene represent the promoter, originally identified from bacteriophage T7, and known to be one of the strongest prokaryotic promoters (*11*). In addition, the translational signals from the start of gene 10 (*12*) from T7 have also been incorporated to allow efficent translation of our synthetic gene. Expression of the synthetic gene is achieved by transferring the plasmid construct to an *E. coli* strain that carries a gene encoding the bacteriophage T7 RNA polymerase (*11*). The T7 RNA polymerase then recognizes its cognate promoter and transcription and translation of the biopolymer gene ensues. Since the biopolymer gene represents a highly repetitive DNA sequence, there is the likelihood that these sequences would rapidly be deleted in the bacterium as a result of homologous recombination. To avoid this possibility, the *recA* mutation that abolishes homologous recombination in *E. coli* , was introduced into the strains used for construction and expression of the biopolymer genes.

For construction of genes encoding the synthetic biopolymers, a set of DNA oligonucleotides were synthesized that encode the various Adeno sequences (Figure 5). In an effort to optimize the expression levels of these sequences, preferred codons for high level expression in *E. coli* were selected for each amino acid. The oligonucleotides coding for the Ad I and Ad III constructs were designed so that upon hybridization of complimentary strands, each double stranded oligonucleotide is left with a two base pair 5' overhang, while the Ad II oligonucleotide left a four base protruding 3' overhang. These overhanging ends allow for insertion of the oligonucleotide into the unique Acc I site of pRHF-1 (Ad I and III) or the unique Ban II site of pRHF-4 (Ad II). In both cases the overhanging ends of the oligonucleotides are nonpalindromic. Two advantages accrue from such a design. First, since we wish to construct multimers of these oligonucleotides, the nonpalindromic sequences allow the monomeric units to be ligated in only a head to tail fashion, thus ensuring that the same coding sequence will simply be repeated. Second, this also ensures that the insertion of the oligonucleotide multimer into the vector can only occur in one orientation.

The oligonucleotides for either Ad I or II were hybridized and ligated to one another to form an assortment of multimers of varying lengths. These were subsequently ligated into the appropriate vector and transformed into the *E. coli* strain DH5D*lac*. Independent ampicillin resistant transformants were grown overnight at 37°C and the plasmid DNA isolated from them. Following cleavage with EcoRI, the plasmid DNA was separated by gel electrophoresis and the size of the inserted oligonucleotide multimer estimated by comparison with the vector DNA containing no insert. Plasmids containing a substantial number of inserts were then transformed into BL21 and tested for expression. Clones pRHF-11 containing 16 repeats of the Ad I sequence, and pRHF-8 containing 26 repeats of the Ad II sequence expressed high levels of a protein of the predicted molecular weight when introduced into BL21.

For the construction of a high molecular weight version of the Ad III sequence, a somewhat different strategy was used. This approach, first reported by Kempe et al. (*13*), is outlined in Figure 6. A single insert of the oligonucleotide is made in pRHF-1. Note that in Figure 5, this oligonucleotide also incorporates two unique restriction enzyme sites, Pvu II and Hpa I. The plasmid DNA containing the

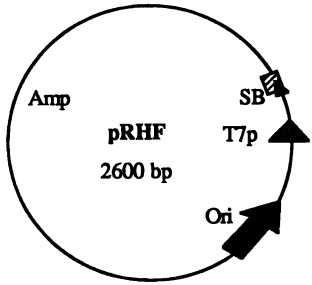

SB = Synthetic Biopolymer Insertion Site

```
          M   A   S   M   T   G   L   L  STOP
     5'                                      3'
pRHF-1 ATG GCT AGC ATG ACT GGT CTA CTG TAG
                           Acc I

          M   A   S   M   T   G   L   L   G   S   G   L   L  STOP
     5'                                                        3'
pRHF-4 ATG GCT AGC ATG ACT GGT CTA CTG GGC TCT GGT CTA CTT TAG
                           Ban II
```

Figure 4. Expression vector design for Ad I and Ad II.


```
Ad I
          L   S   V   Q   T   S   A   P   L   T   V   S   D   G   K
CTG TCT GTT CAG ACC AGC GCG CCG CTG ACC GTT TCC GAC GGT AAG
  C AGA CAA GTC TGG TCG CGC GGC GAC TGG CAA AGG CTG CCA TTC GA

Ad II
          S   G   L   D   F   D   N   N   A   L   R   I   K   L   G
  CT GGT CTG GAC TTT GAC AAC AAC GCT CTG CGT ATC AAG CTG GGC T
CCG AGA CCA GAC CTG AAA CTG TTG TTG CGA GAC GCA TAG TTC GAG

Ad III
          L   Q   L   S   L   R   V   S   E   P   L   D   T   S   H   G   V   N
CTG CAG CTG TCT CTG CGT GTT TCT GAA CCG CTG GAC ACC TCT CAC GGT GTT ACC
  C GTC GAC AGA GAC GCA CAA AGA CTT GGC GAC CTG TGG AGA GTG CCA CAA TTG GA
        ▲                                                       ▲
      Pvu II                                                  Hpa I
```

Figure 5. Nucleotide sequences employed for Ad I, Ad II, and Ad III constructs.

single insert was then cleaved by a combination of either Pst I and Hpa I or Pst I and Pvu II. The appropriate DNA fragments, as outlined in Figure 6, were purified by gel electrophoresis and then religated. As a result of the religation, the insert is now doubled in size. Because the novel joint formed by ligating Pvu II and Hpa I together destroys the sequence recognized by either restriction enzyme, the plasmid is still left with a unique Pvu II and Hpa I site. The process can therefore be repeated again and again each time doubling the size of the insert. Using this method we constructed an Ad III expressing gene containing 64 repeats encoding a protein of ~100,000 mol. wt.

Large scale fermentation runs were done in order to obtain quantites sufficent for physical characterization of the Ad proteins. During overexpression in BL21, all of the Ad proteins formed inclusion bodies with the cell. By isolating the inclusion bodies, a significant factor in purification is gained. Following isolation of the inclusion bodies the pellet was first dissolved in 6 M guanidine hydrochloride followed by exchange with 6 M urea. After a desalting step, the material was passed through a QFF sepharose column and the effluent collected and dialyzed against distilled water. Samples were judged to be better than 90% pure by analyzing samples by SDS-PAGE electrophoresis.

Aggregate Formation in Synthetic Constructs

Dynamic light scattering measurements of particle diffusion coefficients can provide information about the aggregation state of a polymer in solution. Polymer solutions of Ad I (20,000 mol. wt.) were prepared by dissolving lyophilized protein in doubly distilled water which had been filtered through a 0.45 micron pore filter prior to use. Samples were then centrifuged for 20 minutes at 3000g in a refrigerated centrifuge to remove material that may not have dissolved on initial solution formation. Figure 7 shows the concentration dependence of the diffusion coefficient for Ad I solutions, together with the derived value for an apparent molecular particle diameter. The sigmoidal dependence of the viscosity with concentration to produce particles with apparent dimensions larger than 100Å is consistent with the formation of stable fibrillar aggregates at concentrations much lower than used for fiber spinning. These aggregates were observed to stably persist in solution, with slowly increasing size, for several days. Electron microscope examination of these solutions as shown in Figure 8 revealed the presence of long fibrils, behavior also suggested by measurements of the angular dependence of the solution light scattering. Ongoing image analysis of the electron micrographs of these fibrils should be very useful in providing an ultimate definition of their structural organization. It is notable that these aggregates occur in water at substantially lower concentrations than those required for lyotropic mesophase formation in hexafluoroisopropanol (HFIP) used for spinning.

Mesophase Formation and Fiber Spinning(*14*)

The purified proteins Ad I, Ad II, and Ad III were found to be readily soluble in hexafluoroisopropanol (HFIP), a known solvent for polypeptide purification (*15*) and fiber spinning (*16*).

Ad I. Solutions containing 4.7% and 9.6% by weight of Ad I (20,000 mol. wt.) in HFIP were clear and of low viscosity. They were not birefringent when placed between crossed polarizing filters in an optical microscope. A solution containing 14.6% by weight similarly exhibited the non-Newtonian rheological behavior often associated with liquid crystal solutions. On this basis, the 14.6% solution was characterized as isotropic but close to the critical concentration for anisotropy. Solutions of 15.4% and 19.5% by weight of Ad I in HFIP were translucent and more

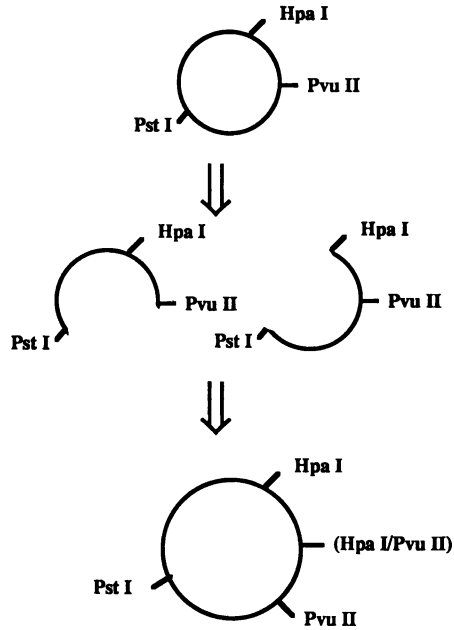

Figure 6. Expression vector strategy for Ad III.

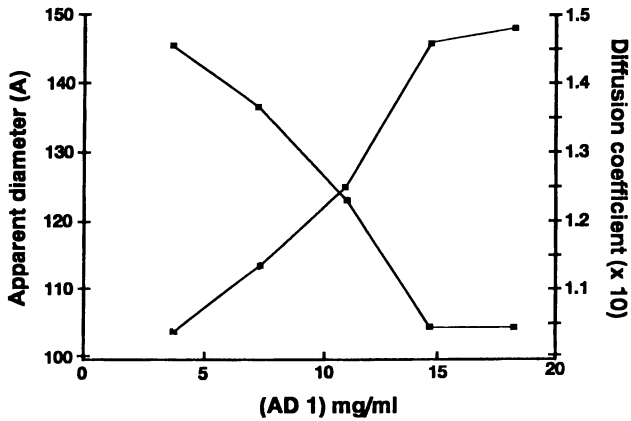

Figure 7. Concentration dependence of solution light scattering of Ad I solutions in water.

viscous with a pronounced shear thinning rheology. Samples viewed between crossed polars were found to be birefringent, showing zones which brightened and darkened as the sample was rotated in the plane of the microscope stage and were judged anisotropic.

Fibers were wet spun from a 19.5% anisotropic solution into methanol. After drying, the 80 denier fibers had a break tenacity of less than one gram/denier and an initial modulus of less than 20 grams/denier. Attempts to increase molecular orientation in the fibers by stretching before drying produced only slight improvements in mechanical properties. Figure 9 depicts the two-step process leading to mesophase formation in Ad I.

Ad II. Ad II (40,000 mol. wt) was observed to be anisotropic above 7.4% solids in HFIP. Although Ad II was soluble in HFIP and capable of forming anisotropic solutions, solubility and liquid crystal formation were improved by the addition of about one part of urea for three parts by weight of protein. In contrast to the borderline anisotropic solution at 7.4% solids, a 7.5% solution of Ad II with 2.5% by weight urea was intensely birefringent and unambiguously liquid crystalline. Urea probably promotes liquid crystal formation by disrupting intermolecular hydrogen bonding and allowing the polymer chains to fold into their minimum energy conformation. Solutions containing up to 19.1% Ad II with 5.5% by weight urea were found to be anisotropic, with rheological properties similar to the 7.5% solution described above.

Ad II fibers were spun from a 7.5% anisotropic solution in HFIP containing 2.2% weight urea into acetone. After drying, the 18 denier fibers had tensile properties similar to those mentioned above for Ad I. Increasing the molecular orientation by stretching the spun fibers 1.5x before drying and then drying under tension yielded 5 denier filaments with a break tenacity of 1.5 grams/denier, a break elongation of 16%, and an initial modulus of 45 grams/denier. Alternatively, hot stretching wet-spun, dried fibers at 200°C allowed a 2.7x stretch and yielded 6 denier fibers with tenacity 1.7 grams/denier, elongation 9%, and modulus 39 grams/denier.

Fibers were also spun from 7.4% mesophase solutions in HFIP without urea. After drying, the fibers were drawn 3x at room temperature producing 18 denier filaments with tenacity 2.6 grams/denier, elongation 30%, and modulus 38 grams/denier. These mechanical properties are comparable to those of several commercial textile fibers.

Ad III. Solutions of Ad III (100,000 mol. wt.) in HFIP were found to be isotropic, even at polymer concentrations as high as 15% by weight. Solutions of up to 15% Ad III in strong polar solvents, such as dichloroacetic acid and aqueous lithium thiocyanate, similarly showed no signs of anisotropy. We attribute this behavior to electrostatic repulsion between ionizable groups in the side chains in the Ad III construct preventing the polymer from folding as required to form the fibrillar aggregates necessary for phase separation.

Ad III fibers were spun from 15% by weight isotropic solutions in HFIP into methanol. Only modest tensile properties were achieved from the isotropic solutions similar to those obtained for Ad I.

Structural Characterization of Polymers/Fibers

Structural analysis via X-ray diffraction of Ad I, II, and III is summarized in Figure 10 which gives the powder diffraction patterns from compressed, dry powders. All three patterns are similar with reflections at 1.02nm and 0.47nm (see Table 1) and a broad scattering feature at 0.38nm. The reflection at 0.47 nm, while not observed by Devaux et al.(*6*) in adenovirus fiber crystals, is direct evidence for the presence of a β-

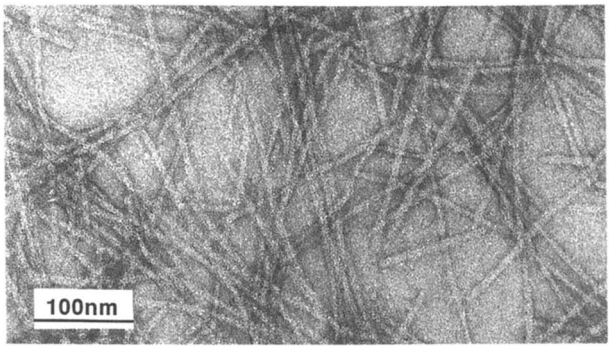

Figure 8. Ad I fibrillar aggregates. Solution was deposited on a carbon-coated copper mesh grid, stained with 1% uranyl acetate and imaged with a Hitachi 6000 electron microscope at 100 KV.

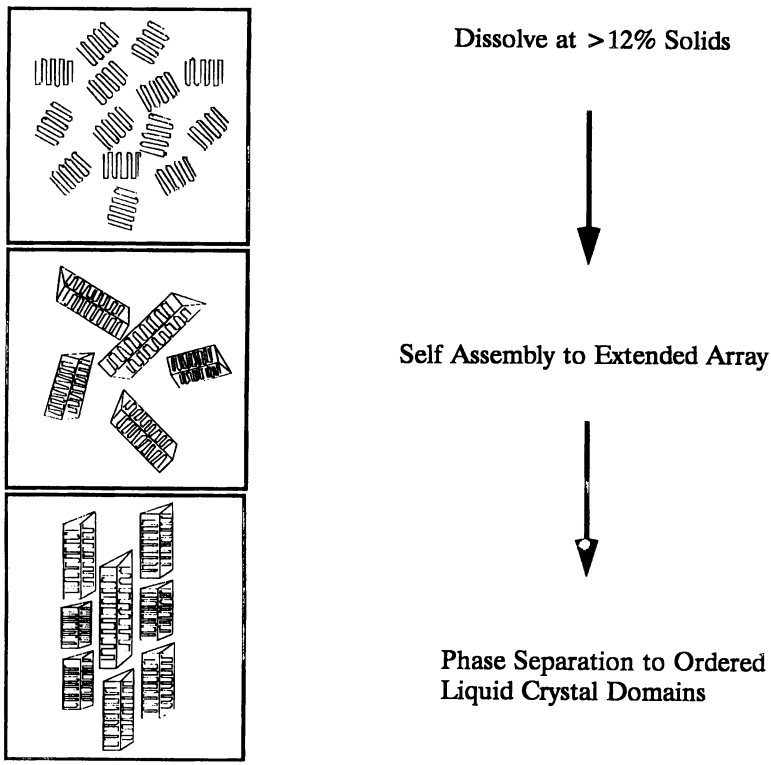

Figure 9. Mesophase formation in Ad I. Self-assembly to rodlike aggregates precedes phase separation above the critical concentration of 12% solids.

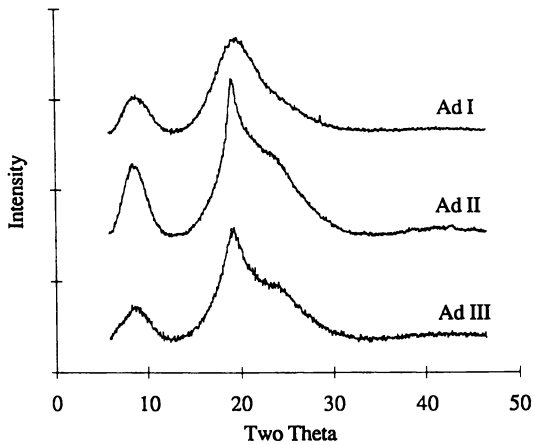

Figure 10. Powder diffraction patterns for dry adenovirus constructs.

sheet structure in these constructs. The peak is associated with the chain separation distance within the hydrogen bonded β-sheet. The absence of additional reflections in the diffraction patterns suggests that the sheets are assembled in a non-standard manner. The diffraction data also show that Ad II and Ad III have more highly developed sheets, possibly due to their higher molecular weight and/or their different composition for the fold region compared to Ad I. Diffraction patterns were obtained from fibers of the different adeno constructs described above. In general, the molecular orientation in these fibers was not sufficient to allow a determination of cross β-structure. Samples stored at high relative humidities and/or freshly prepared from water solutions show an additional reflection at 2.25nm which disappears when the samples are heat-treated and/or dried extensively. This behavior suggests that water is an integral part of the ordered structure.

Table I. X-ray diffraction spacings for Ad I, II, III

Dry			Wet	
Ad I	Ad II	Ad III	Ad I	Ad III
			2.241	2.250
1.000	1.023	1.022	1.022	1.018
0.461	0.466	0.466	0.466	0.469
0.377	0.397	0.380	0.384	2.250

The unique nature of the organization versus conventional β-silks is supported by thermal measurements. The DSC traces of these materials are characterized by a sharp melting endotherm at 219°C. In contrast, native silks melt at or above 300°C.

Conclusions

The work described in this paper represents a complete iteration through a design, synthesis, fabrication and evaluation cycle for precision protein polymer synthesis. The results have shown that it is possible through precise specification of molecular level parameters, such as polymer sequence and composition, to control both material architecture and processibility for possible downstream manufacturing operations. The facile, self-assembly of the simplified synthetic adenovirus constructs described above into sophisticated, highly ordered structures provides encouragement to the materials scientist interested in capturing the efficiency and utility of evolutionary building blocks present in natural materials. In some cases, we expect that the design and synthesis of simplified synthetic analogs to such natural structures will lead to materials which outperform their natural counterparts in applications where biologically imposed material constraints are unimportant.

Acknowledgments

The authors wish to thank Mr. Don Smith for protein purification, Dr. Richard A. Yates for fermentation development, and Dr. Catheryn L. Jackson for the electron microscopy.

Literature Cited

(1) Valentine, R. C.; Pereira, H. G. *J. Mol. Biol.* **1965**, *13*, pp. 13-22.
(2) Sundquist, B.; Pettersson, U.; Thelander, L.; Phillipson, L. *Virology* **1973**, *51*, pp. 252-256.
(3) Devaux, C.; Zulauf, M.; Boulanger, P.; Jacrot, B., *J. Mol. Biol.* **1982**, *156*, pp. 927-937.

(4) Green, N. M.; Wrigley, N. G.; Russel, W. C.; Martin, S. R.; McLachlan, A. D. *EMBO* **1983**, *2*, No. 8, pp 1357-1365.
(5) Stouten, F. W.; Sander, C., *J. Mol. Biol.* **1992**, *220*, pp. 1073-1084.
(6) Devaux, C.; Adrian, M.; Berthet-Columinas, C.; Cusack, S; Jairot, B., *J. Mol. Biol.* **1990**, *215*, pp. 567-588.
(7) Herisse, J.; Galibert, F. *Nucleic Acids Res.* **1981**, *9*, pp. 1229-1240.
(8) Herisse, J.; Rigolet, M.; deDinechin, S. D.; Galibert, M. *Nucleic Acids Res.* **1981**, *9*, pp. 4023-4042.
(9) Chatellard, C.; Chroboczek, J. *Gene* **1989**, *81*, pp. 267-274.
(10) Albiges-Rizo, C.; Chroboczek, J. *J. Mol. Biol.* **1990**, *212*, pp. 247-252.
(11) Studier, F. W.; Moffatt, B. A. *J. Mol. Biol.* **1986** *189*, pp. 113-130.
(12) Olins, P. O.; Devine, C. S.; Rangwala, S. H.; Kavka, K. S. *Gene* **1988** *73*, pp. 227-235.
(13) Kempe, T.; Kent, S. B. H.; Chow, F.; Peterson, S. M.; Sundquist, W. I.; L'Italien, J. J.; Harbrecht, D.; Plunkett, D.; DeLorbe, W. J. *Gene* **1985** *39*, pp. 239-245.
(14) Hoess, R. H.; O'Brien, J. P; Salemme, F. R. Internat. Pat. Appl., WO 92/09695, 1992.
(15) Hayashi et al., U.S. Patent No. 4,594,409.
(16) Lock, U.S. Patent No. 5,171,505.

RECEIVED May 4, 1993